Structure and characteristics of ultrathin indium tin oxide films

Er-Jia Guo, Haizhong Guo, Huibin Lu,[a] Kuijuan Jin, Meng He, and Guozhen Yang
Beijing National Laboratory for Condensed Matter Physics, Institute of Physics, Chinese Academy of Sciences, Beijing 100190, People's Republic of China

(Received 29 November 2010; accepted 20 December 2010; published online 4 January 2011)

A series of indium tin oxide (ITO) thin-films with various thicknesses from 2 to 200 monolayers (ML) have been epitaxially grown on $LaAlO_3$ substrates by laser molecular-beam epitaxy. The measurements of x-ray diffraction, atomic force microscopy, four-probe method, and optical transmittance reveal that the film thickness strongly affects the structural, electrical, and optical properties of ITO thin-films, and the ITO thin-films exist at a critical thickness of metal-insulator transition at about 4–5 ML. The electrical transport property has been discussed with the different conductive models. © *2011 American Institute of Physics*. [doi:10.1063/1.3536531]

Transparent conducting oxide films have been extensively studied in recent years because they not only exhibit high optical transparency in the visible range but also possess high electrical conductivity.[1] They are expected to serve as the detection windows for the optoelectronic devices. Indium tin oxide (ITO) with a wide band gap of ~3.8 eV and high transparency (>80%) in the visible range[2] has attracted considerable attention due to its great potential applications for antistatic coatings, flat panel displays, solar cells, defrosters, and optical coatings.[3–5] From the application point of view, the structure and surface roughness as well as the scale effect are very important, especially, for the ultrathin oxide films. However, only a few works focused on the properties of ultrathin ITO films. Kim *et al.*[6] fabricated ITO films on a plastic substrate and studied the electrical properties with the thickness of 40–280 nm, Gao *et al.*[7] and Hao *et al.*[8] studied the thickness effect on physical properties of ITO films in the thickness range from 15 to 103 nm and from 72 to 447 nm, respectively. In this letter, we report the thickness dependence of the structural, electrical, and optical properties of epitaxial ITO thin-films with a thickness range from 2 to 200 monolayers (ML). The experimental results show that the structure and the physical properties of ITO thin-films are strongly dependent on the film thickness.

A series of ITO thin-films with various thicknesses of 2, 4, 5, 10, 20, 30, 50, 100, and 200 ML were epitaxially grown on $LaAlO_3$ (LAO) (001) substrates using a sintered ceramic ITO (In_2O_3:SnO_2=90:10 wt %) target by laser molecular-beam epitaxy (MBE).[9] The preparation conditions are as follows: the pulsed XeCl excimer laser with a wavelength of 308 nm has a repetition rate of 2 Hz, the energy density was ~1.5 J/cm^2, the LAO substrate temperature was kept at 680 °C, and an oxygen pressure of 1.5×10^{-1} Pa with ~20% O was maintained throughout the deposition. After the deposition, the samples were *in situ* annealed under the growth conditions for 30 min. The thickness of ITO thin-films was monitored by an *in situ* reflection high-energy electron diffraction intensity oscillations, which displayed the growth rate of about 1 ML ITO per 25 laser pulses, and further confirmed by an *ex situ* surface profile measuring system.

The structure of ITO thin-films was analyzed by x-ray diffraction (XRD) θ-2θ scan and φ scan. Figure 1(a) shows typical XRD θ-2θ curves of 5, 10, 20, 30, 50, and 200 ML ITO thin-films grown on LAO substrate. The patterns only show the peaks corresponding to (00*l*) reflections of ITO thin-films and LAO substrates, indicating that the ITO thin-films were epitaxially grown on LAO substrates. The ITO (004) diffraction peak gradually becomes broader with the

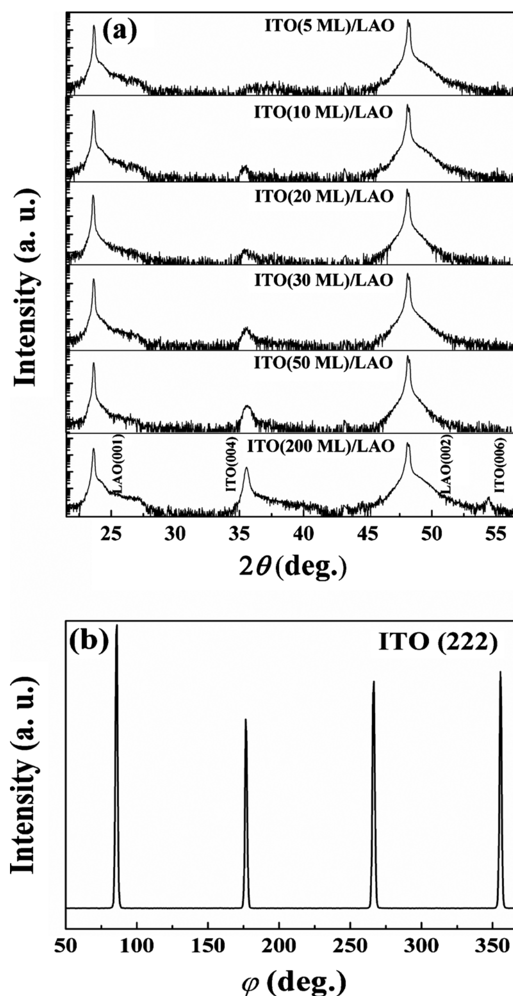

FIG. 1. (a) The XRD spectra of 5, 10, 20, 30, 50, and 200 ML ITO thin-films grown on LAO. (b) φ scan of ITO (222) diffraction peak of 200 ML ITO thin-film.

[a]Author to whom correspondence should be addressed. Electronic mail: hblu@aphy.iphy.ac.cn.

 © 2011 American Institute of Physics

Author complimentary copy. Redistribution subject to AIP license or copyright, see http://apl.aip.org/apl/copyright.jsp

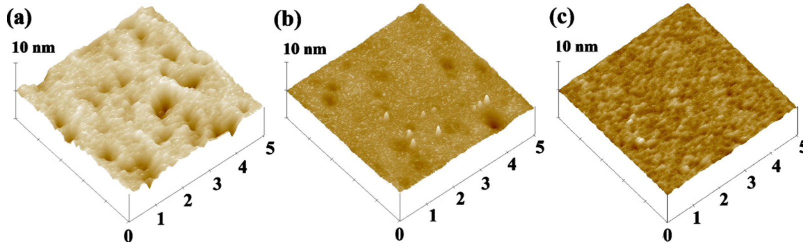

FIG. 2. (Color online) AFM 3D images (5×5 μm^2): (a) 5, (b) 20, and (c) 200 ML ITO thin-films grown on LAO substrates.

decrease of the film thickness, which could be attributed to the lattice mismatch and size effect. Figure 1(b) is the φ scan of ITO (222) diffraction peak of 200 ML ITO thin-film at a constant, $\psi=55.13°$. The 2θ angle was fixed for the ITO (222) diffraction peak, $2\theta=30.562°$. Four sharp discrete peaks reveal that the ITO thin-film is a fourfold rotational symmetry.

Figures 2(a)–2(c) show three typical atomic force microscopy (AFM) images of ITO thin-films with thicknesses of 5, 20, and 200 ML, respectively. The root-mean-square surface roughnesses are 1.886, 1.651, 0.929, 0.775, and 0.315 nm for 5, 10, 20, 50, and 200 ML ITO thin-films within a 5×5 μm^2 area, respectively. There are some hollows in the 5 ML ITO thin-film, and the hollow depth measured is ~4.09 nm approaching the film thickness of ~5 nm. As shown in Fig. 2(b), 20 ML ITO thin-film presents a smoother surface compared with 5 ML ITO in Fig. 2(a). With further increasing the film thickness, the surface of 200 ML ITO thin-film becomes atomically smooth. The results suggest that the ITO thin-films form three-dimensional (3D) islands at the early growth, and then the island diameter turns larger and gradually coalesces with increasing film thickness. Finally, the surface of ITO thin-film became atomic scale smooth.

The electrical transport properties of the ITO films were measured by the four-probe method in a temperature range of 4.2–300 K with a superconducting quantum interference device. Figures 3(a)–3(e) show the temperature dependence of the resistivities (ρ) for the ITO thin-films of 200, 50, 20, 10, and 5 ML, respectively. The ρ-T curves could not be measured when the ITO thin-films are below 4 ML due to the high values of the resistance. From Figs. 3(a)–3(e), we can see that the ITO thin-films with a thickness above 10 ML present a metal-insulator (M-I) transition with decreasing the temperature. The transition temperatures (T_C), increasing with the decrease of the film thicknesses, are about 94, 96, 190, and 222 K for 200, 50, 20, and 10 ML ITO thin-films, respectively. As shown in Fig. 3(e), the 5 ML ITO thin-film presents a semiconducting property in the temperature range of 4.2–300 K. Figure 3(f) shows the variation of resistivity with the ITO film thicknesses measured at 300 K. The resistivities are 8.68×10^{-5}, 4.32×10^{-4}, 2.75×10^{-3}, 1.16×10^{-2}, 9.46×10^{-2}, 8.86×10^{3} and 2.11×10^{4} Ω cm for the ITO thin-films of 200, 50, 20, 10, 5, 4, and 2 ML at room temperature, respectively. They are the lowest resistivity in the literature with the similar thickness, attributed to the high-quality epitaxial ITO thin-films. The electron mobilities are 39.2, 26.5, 2.94, 1.56, and 0.813 cm^2/V s for 200, 50, 20, 10, and 5 ML ITO thin-films measured by Hall measurements at 300 K, respectively. In the inset of Fig. 3(f), we show a phase diagram of T_C with the film thickness. The variation of T_C with thickness is in agreement with that of the resistivity. Similar to $SrRuO_3$ thin-films,[10,11] the resistivity and T_C have a rapid enhancement when the ITO thin-film is below 5 ML, indicating that the critical thickness of ITO thin-film is about 4–5 ML, and the physical properties are strongly influenced by the microstructure and the film thickness.

The electronic transport property is related to the structure, especially for the ultrathin films. We study the mechanism of the transport property of ITO films with the conductive model of two dimensions and three dimensions. For the ITO thin-films with a thickness above 5 ML, we consider that the electric transport properties are much close to the 3D weak localization model, and the temperature dependence of the resistivity can be described by[12,13]

$$\frac{1}{\rho(T)} = \frac{1}{\rho_0} + \frac{e^2}{\hbar \pi^3 a} T^{1/2}, \tag{1}$$

where ρ_0 is the residual resistivity due to impurity scattering, e is the charge of one electron, $\hbar$ is the Planck constant, a is the coefficient, and T is the measuring temperature. Figure 4(a) presents the relationship between $1/\rho$ and $T^{1/2}$ for the ITO thin-films of 200, 50, 20, and 10 ML. The solid lines in Fig. 4(a) are simulated from Eq. (1). The well linear relation between $1/\rho$ and $T^{1/2}$ can be obtained at temperature range from about 5 to 100 K, suggesting that the mechanism of

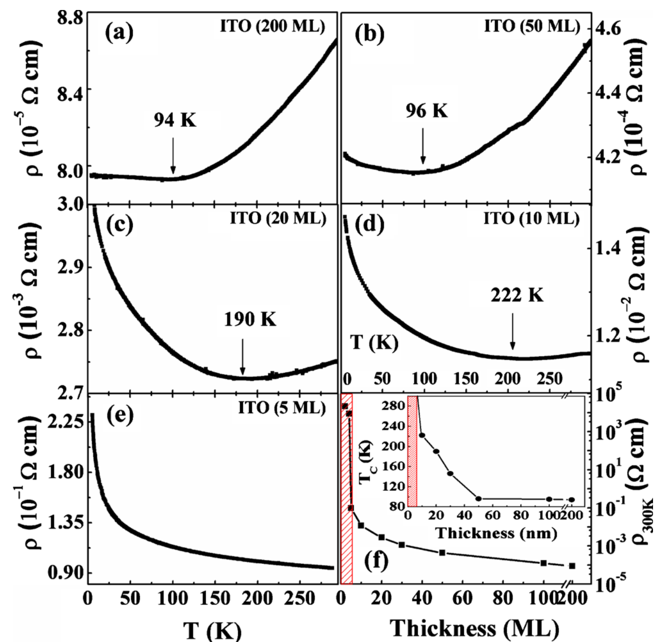

FIG. 3. (Color online) The temperature dependence of resistivity (ρ) for the ITO thin-films with various thicknesses: (a) 200, (b) 50, (c) 20, (d) 10, and (e) 5 ML. The film thickness dependence of the resistivity of ITO films at 300 K is shown in (f). Inset in (f) is a phase diagram of ITO thin-films showing the relationship between transition temperature T_C and the film thickness. The red hatched areas in (f) represent the insulator states of ITO films with thickness below 5 ML.

Author complimentary copy. Redistribution subject to AIP license or copyright, see http://apl.aip.org/apl/copyright.jsp

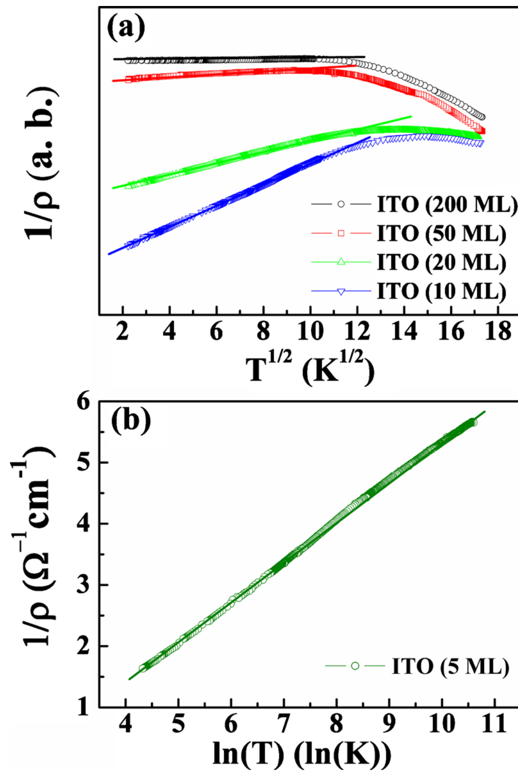

FIG. 4. (Color online) (a) The relationship between $1/\rho$ and $T^{1/2}$ for the ITO thin-films of 200, 50, 20, and 10 ML. (b) The relationship between $1/\rho$ and $\ln T$ for the 5 ML ITO thin-film. The solid lines in (a) and (b) are simulated from Eqs. (1) and (2), respectively.

electronic transport for ITO thin-films with thicknesses above 5 ML obeys 3D weak localization model.

For the ITO films with 5 ML, two-dimensional (2D) localization model can be used to explain the transport property, and the resistivity can be described as follows:[10,14]

$$\frac{1}{\rho(T)} = \frac{1}{\rho_0} + a \ln T, \tag{2}$$

where ρ_0 is the residual resistivity due to impurity scattering, a is the coefficient, and T is the measuring temperature. Figure 4(b) shows the relationship between $1/\rho$ and $\ln T$ for the 5 ML ITO thin-film. The experimental data of the 5 ML ITO film show a good linear fitting with the solid line simulated from Eq. (2), suggesting that the ITO thin-films with below 5 ML will result in a very large resistivity, and the transport behavior follows the 2D localization model. The results can be also confirmed by the AFM images in Fig. 2. The 2D conduction model plays a major role in the transport mechanism because the ultrathin ITO films exhibit 3D islands and deep trenches. When the film thickness increases, the islands and trenches gradually coalesced, and the film surface becomes smooth, the role of size effect becomes weak, and 3D localization dominates in the transport properties.

Figure 5 presents the optical transmittances of ITO films. The transmittances are about 9%, 63%, and 76% in 280 nm wavelength for the 100, 20, and 5 ML ITO films, respectively. The 100 ML ITO thin-film shows a sharp cutoff wavelength at about 320 nm, agreeing well with the ITO band gap of 3.8 eV.[2] With the decrease of the thickness of ITO film, the absorption of deep-ultraviolet (DUV) light in ITO film decreased. From Figs. 3 and 5, we can see that the ITO

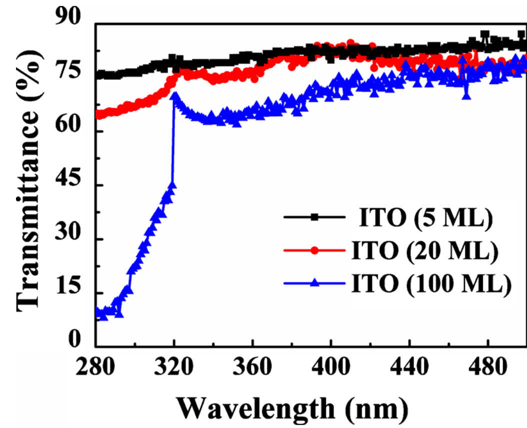

FIG. 5. (Color online) Optical transmittances of ITO thin-films with thicknesses of 5, 20, and 100 ML.

thin-films with 5–10 ML have not only a well conductive property but also a high transmittance of DUV light. We have fabricated low-noise solar-blind photodetectors with LAO single crystal using 5 ML ITO as the electrode and detection window.[15]

In conclusion, the high-quality ultrathin ITO thin-films with a thickness ranging from 2 to 200 ML have epitaxially grown on LAO substrates by laser MBE. The studies prove that the film thickness strongly affects the structural, electrical, and optical properties of ITO thin-films. The ITO thin-films exist at a critical thickness of *M-I* transition at about 4–5 ML and show quite well conductive property at room temperature when the thickness is more than 4 ML. The ITO thin-films with 5–10 ML have a well conductive property and high transmittance of DUV light. The results suggest that the ultrathin ITO films as transparent electrodes and windows have potential applications in the optoelectronic devices.

This work was supported by the National Basic Research Program of China and the National Natural Science Foundation of China.

[1]J. F. Wager, Science **300**, 1245 (2003).
[2]W. S. Jahng, A. H. Francis, H. Moon, J. I. Nanos, and M. D. Curtis, Appl. Phys. Lett. **88**, 093504 (2006).
[3]F. Li, H. Tang, and J. Shinar, Appl. Phys. Lett. **70**, 2741 (1997).
[4]O. N. Mryasov and A. J. Freeman, Phys. Rev. B **64**, 233111 (2001).
[5]K. Nomura, H. Ohta, K. Ueda, T. Kamiya, M. Hirano, and H. Hosono, Science **300**, 1269 (2003).
[6]D. H. Kim, M. R. Park, H. J. Lee, and G. H. Lee, Appl. Surf. Sci. **253**, 409 (2006).
[7]M. Z. Gao, R. Job, D. S. Xue, and W. R. Fahrner, Chin. Phys. Lett. **25**, 1380 (2008).
[8]L. Hao, X. Diao, H. Xu, B. Gu, and T. Wang, Appl. Surf. Sci. **254**, 3504 (2008).
[9]H. B. Lu, K. J. Jin, Y. H. Huang, M. He, K. Zhao, B. L. Cheng, Z. H. Chen, Y. L. Zhou, S. Y. Dai, and G. Z. Yang, Appl. Phys. Lett. **86**, 241915 (2005).
[10]G. Herranz, B. Martínez, J. Fontcuberta, F. Sánchez, C. Ferrater, M. V. García-Cuenca, and M. Varela, Phys. Rev. B **67**, 174423 (2003).
[11]D. Toyota, I. Ohkubo, H. Kumigashira, M. Oshima, T. Ohnishi, M. Lippmaa, M. Takizawa, A. Fujimori, K. Ono, M. Kawasaki, and H. Koinuma, Appl. Phys. Lett. **87**, 162508 (2005).
[12]P. A. Lee and T. V. Ramakrishnan, Rev. Mod. Phys. **57**, 287 (1985).
[13]E. Abrahams, P. W. Anderson, D. C. Licciardello, and T. V. Ramakrishnan, Phys. Rev. Lett. **42**, 673 (1979).
[14]Y. Z. Chiou and J. J. Tang, Jpn. J. Appl. Phys., Part 1 **43**, 4146 (2004).
[15]E. J. Guo, H. B. Lu, M. He, K. J. Jin, and G. Z. Yang, Appl. Opt. **49**, 5678 (2010).

Author complimentary copy. Redistribution subject to AIP license or copyright, see http://apl.aip.org/apl/copyright.jsp